

# INFLUENCE OF GEOMETRIC PARAMETERS OF A PIN JOINT OF A CARBON/EPOXY COMPOSITE PLATE ON ITS LOAD CAPACITY

## VPLIV GEOMETRIJSKIH PARAMETROV NA NOSILNOST ZATIČNEGA SPOJA KOMPOZITNE PLOŠČE OGLJIKOVA VLAKNA-EPOKSI

Jan Krystek<sup>1</sup>, Lukáš Bek<sup>2</sup>, Tomáš Kroupa<sup>1</sup>, Radek Kottner<sup>1</sup>

<sup>1</sup>University of West Bohemia, NTIS – New Technologies for the Information Society, Univerzitní 22, 306 14 Plzeň, Czech Republic

<sup>2</sup>University of West Bohemia, Department of Mechanics, Univerzitní 22, 306 14, Plzeň, Czech Republic  
krystek@kme.zcu.cz

Prejem rokopisa – received: 2013-10-01; sprejem za objavo – accepted for publication: 2014-01-08

The influence of geometric parameters of a composite pin joint on its load capacity was investigated. Numerical simulations of the pin joint were performed using the finite-element method in Abaqus. A material model with non-linear dependence of the shear stress/strain was used. A progressive-failure model was used in these simulations. The numerical model was validated by means of a comparison of experimental and numerical results. The behaviour of the pin joint was then further investigated using a calibrated FE model.

Keywords: CFRP, Hashin criterion, finite-element method, load capacity, pin joint, progressive failure

Preiskovan je bil vpliv geometrijskih parametrov kompozitnega zatičnega spoja na njegovo nosilnost. Numerična simulacija zatičnega spoja je bila izvršena z uporabo metode končnih elementov na Abaqusu. Uporabljen je bil model materiala z nelinearno odvisnostjo strižna napetost – raztezek. V tej simulaciji je bil uporabljen model postopnega popuščanja. Numerični model je bil ocenjen s primerjavo eksperimentalnih in numeričnih rezultatov. Vedenje zatičnega spoja je bilo nato preiskano z uporabo kalibriranega FE-modela.

Ključne besede: CFRP, Hashinov kriterij, metoda končnih elementov, nosilnost, zatični spoj, postopno popuščanje

## 1 INTRODUCTION

Currently, the scope of the products that utilize composite materials is rapidly increasing. Usually, not the whole structure is replaced with composite materials, but only a certain part of it is replaced. However, the integration of a composite part into a metal structure brings many problems, especially the ones related to joints. Using pin joints is one possibility of joining composites with metals. Typical failure mechanisms of a

composite in a pin joint are shown in **Figure 1**. The type of failure depends on the geometry of the composite part and on the type of the composite (materials of constituents, lay-up, etc.)<sup>1</sup>.

An experimental analysis and numerical prediction of the influence of geometric parameters of a pin joint of a composite plate on its load capacity is the aim of this work.

## 2 EXPERIMENT

The tested specimens were cut using water jet from the plates made of 8 pairs of prepreg layers. The pin holes were milled. The carbon-fibre-reinforced plastic (CFRP) consisted of Tenax HTS 5631 high-strength fibres and epoxy resin.

Investigated geometric parameters of the specimens are shown in **Figure 2**, where  $D$  is the hole diameter,  $W$  is the width of the specimens,  $E$  is the distance from the centre of the hole to the free end,  $H$  is the thickness,  $Q_E$  and  $Q_W$  are the side widths:

$$Q_E = E - \frac{D}{2}; \quad Q_W = \frac{W - D}{2} \quad (1)$$

The hole diameter was  $D = 8$  mm, the thickness  $H = 2.3$  mm,  $E/D = \{1, 2, 3, 4, 5\}$ ,  $W/D = \{2, 3, 4, 5\}$ . Stacking sequence  $[0_2/-45_2/45_2/90_2]_s$  was analyzed.

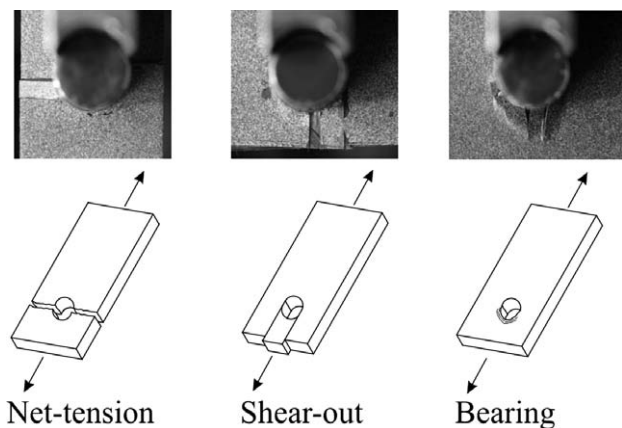


Figure 1: Typical failure mechanism of a composite pin joint  
Slika 1: Značilen mehanizem poškodbe kompozitnega zatičnega spoja

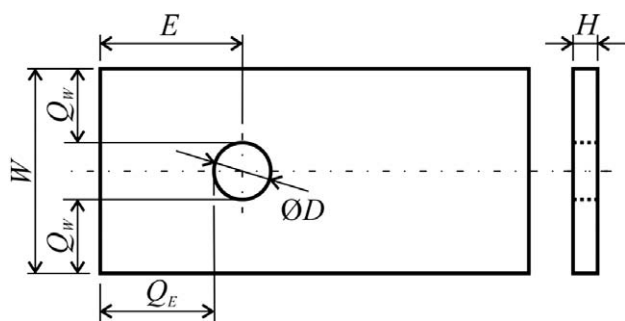


Figure 2: Investigated geometric parameters  
Slika 2: Preiskovani geometrijski parametri

The experimental set-up is shown in Figure 3. A special experimental device that allowed us to monitor all the visible changes of the experimental specimens with two cameras was designed. This device was installed into a Zwick/Roell Z050 testing machine. The specimens were tested in tension in the axial direction (Figure 2). The loading speed was  $v = 0.5$  mm/min.

Experimental dependencies of the specimen load capacity on the  $E/D$  and  $W/D$  ratios are presented in Figures 4 and 5. The load capacity of the joint corresponds to the maximum force  $F_{max}$  (the final failure occurs under  $F_{max}$ ). It is obvious that the load capacity in the case of the shear-out-failure mechanism was mainly lower than in the case of the bearing-failure mechanism. The bearing strength did not increase with the increasing geometric ratios  $E/D$  and  $W/D$ . The ultimate failure did not occur in the case of the bearing-failure mechanism.

### 2.1 Numerical simulations

Mechanical properties of the composite were identified using tensile and compressive tests<sup>2</sup>. Non-linear dependence of the shear stress/strain was considered. A progressive failure model<sup>3,4</sup> was used for the prediction of the final failure of the specimens. Due to non-linear behaviour of the used composite, the shear stresses were calculated from these equations:

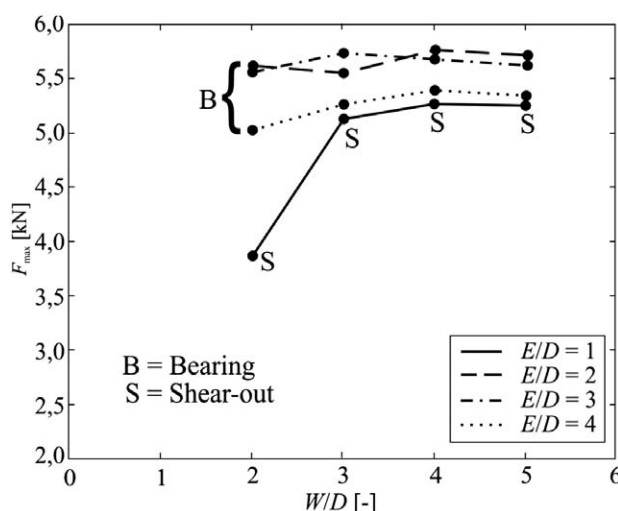


Figure 4: Load capacity of the pin-jointed  $[0_2/-45_2/45_2/90_2]_s$  laminate  
Slika 4: Nosilnost zatičnega spoja  $[0_2/-45_2/45_2/90_2]_s$  laminata

$$\sigma_{12}(\gamma_{12}) = \frac{G_{12}^0 \cdot \gamma_{12} (1 - d_{12})}{\left[ 1 + \left( \frac{G_{12}^0 \cdot \gamma_{12}}{\tau_{12}^0} \right)^{n_{12}} \right]^{\frac{1}{n_{12}}}} \quad (2)$$

$$\sigma_{13}(\gamma_{13}) = \frac{G_{12}^0 \cdot \gamma_{13} (1 - d_{12})}{\left[ 1 + \left( \frac{G_{12}^0 \cdot \gamma_{13}}{\tau_{12}^0} \right)^{n_{12}} \right]^{\frac{1}{n_{12}}}}$$

where  $d_{12}$  is the damage variable. Value  $d_{12} = 0$  denotes the undamaged material and value  $d_{12} = 1$  denotes the total damaged material in this point. The damage of the material occurs when the failure criterion predicts failure.

The elements of the stiffness matrix can be calculated from the following relation:

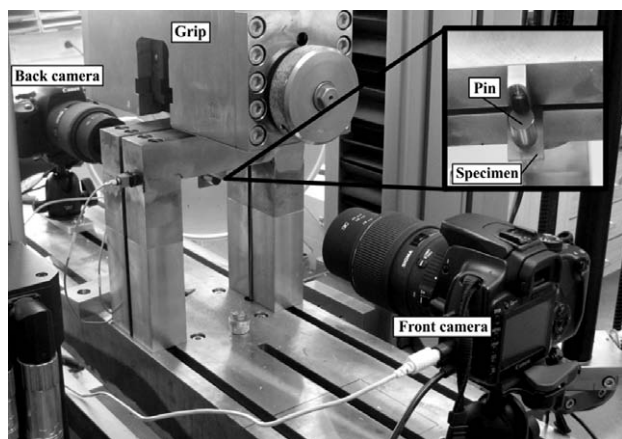


Figure 3: Experimental set-up  
Slika 3: Eksperimentalni sestav

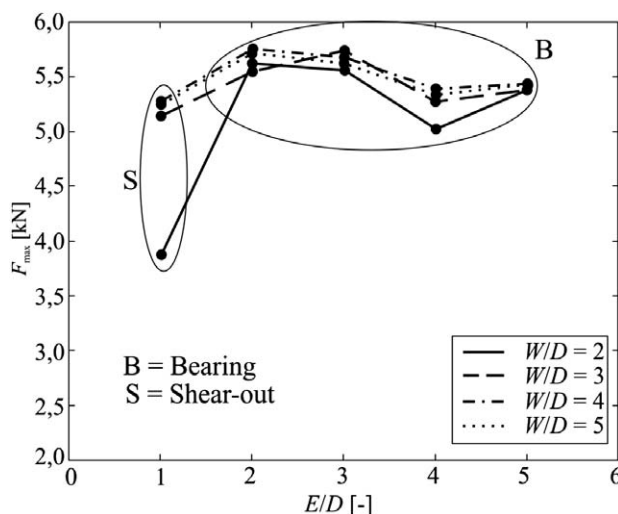


Figure 5: Load capacity of the pin-jointed  $[0_2/-45_2/45_2/90_2]_s$  laminate  
Slika 5: Nosilnost zatičnega spoja  $[0_2/-45_2/45_2/90_2]_s$  laminata

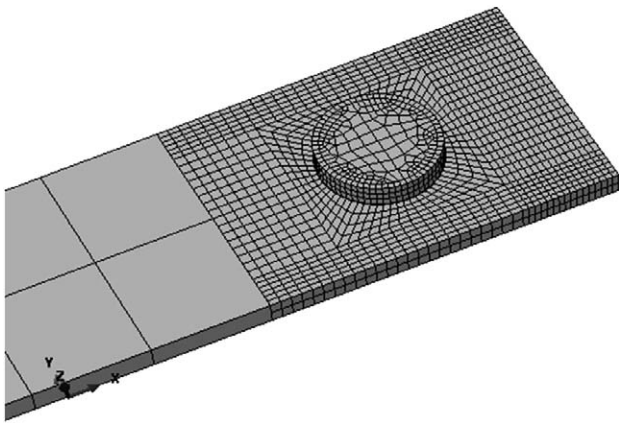


Figure 6: Mesh of the model  
Slika 6: Mreža modela

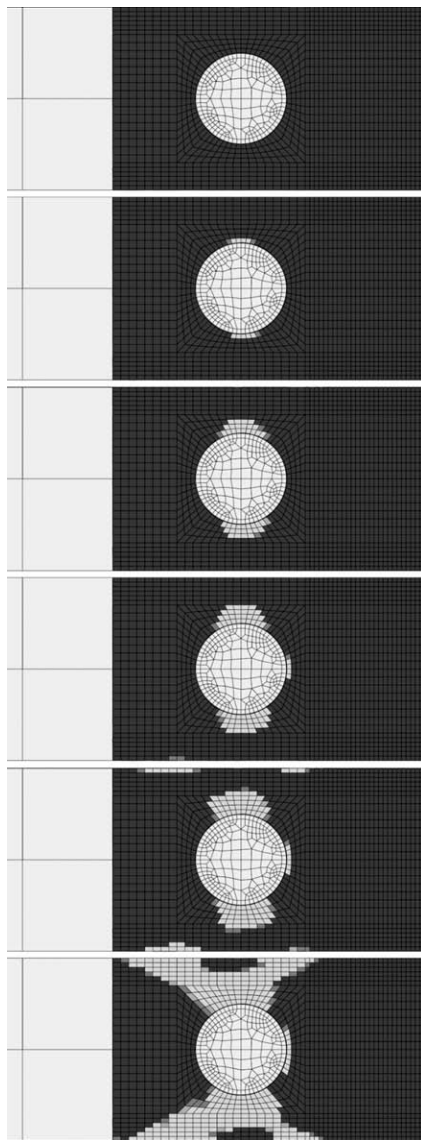


Figure 7: Progress of damage in the 90° layer (black – undamaged, grey – damaged),  $D = 8$  mm,  $E = 16$  mm,  $W = 16$  mm  
Slika 7: Napredovanje poškodbe v plasti 90° (črno – nepoškodovano, sivo – poškodovano),  $D = 8$  mm,  $E = 16$  mm,  $W = 16$  mm

$$C_{ij} = \frac{\partial \sigma_{ij}}{\partial \epsilon_{ij}} \quad (3)$$

The identified mechanical properties of the composite material are presented in Table 1.

Table 1: Mechanical properties of the investigated composite plate<sup>2</sup>  
Tabela 1: Mehanske lastnosti preizkušane kompozitne plošče<sup>2</sup>

Parameter	Units	Value	Parameter	Units	Value
$E_1$	GPa	116.2	$X^T$	MPa	1800
$E_2$	GPa	11.5	$X^C$	MPa	850
$\mu_{12}$	–	0.395	$Y^T$	MPa	55
$G_{12}^0$	GPa	5.0	$Y^C$	MPa	213
$\tau_{12}^0$	MPa	27.2	$S^L$	MPa	82
$n_{12}$	–	0.33			

The Abaqus finite-element system was used for the numerical simulation. A parametrically made model was created using linear, layered brick elements for the composite plate and linear brick elements for the steel pin. The mesh of the model is obvious from Figure 6. The composite laminae were assumed as transversally isotropic, homogeneous and non-linearly elastic. The friction between the composite and steel pin was neglected. The steel pin joint was modelled as a linear isotropic material ( $E_s = 210$  GPa,  $\mu_s = 0.3$ ).

Hashin failure criterion<sup>5</sup> was used for the prediction of failure. The non-linear model and the progressive failure model were included in the Abaqus system using the UMAT subroutine. The progress of joint damage in the case of a layer with a fibre angle of 90° is shown in Figure 7.

### 3 RESULTS

The maximum discrepancy between the experimental and numerical results was 22 %, the average discrepancy was 13 %. Result dependencies of the load capacity obtained from numerical simulations are obvious from Figures 8 to 11.

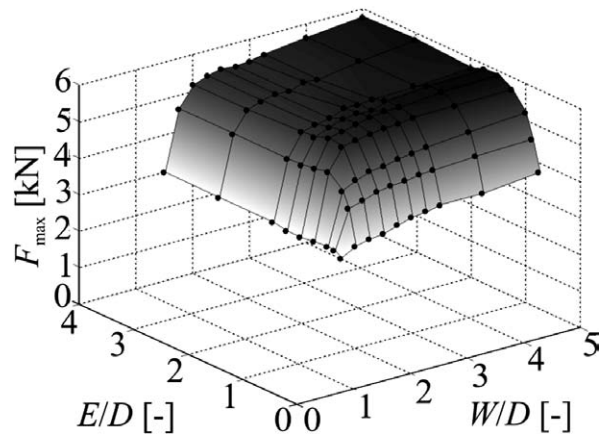
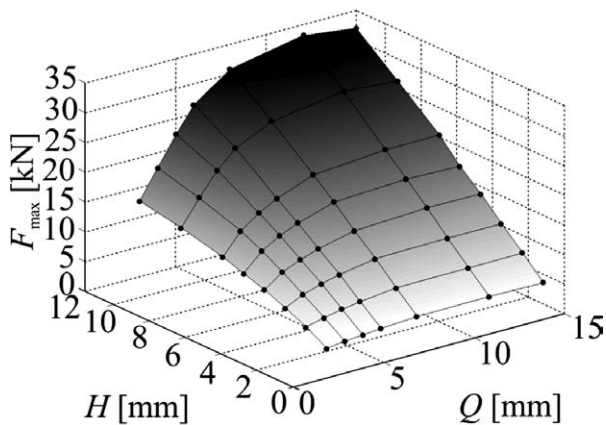
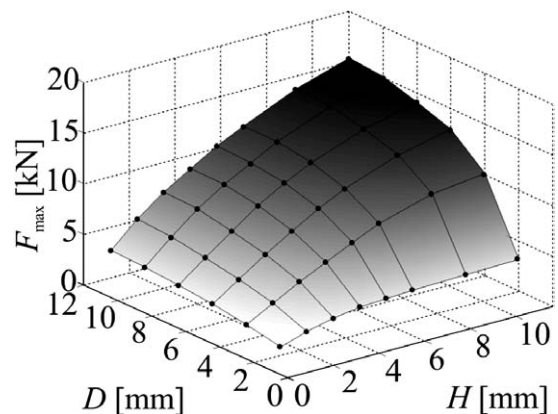


Figure 8: Load capacity of the pin joint for  $D = 8$  mm and  $H = 2.3$  mm

Slika 8: Nosilnost zatičnega spoja za  $D = 8$  mm in  $H = 2,3$  mm



**Figure 9:** Load capacity of the pin joint for  $D = 10$  mm  
**Slika 9:** Nosilnost zatičnega spoja za  $D = 10$  mm



**Figure 11:** Load capacity of the pin joint for  $Q = 3.5$  mm  
**Slika 11:** Nosilnost zatičnega spoja za  $Q = 3,5$  mm

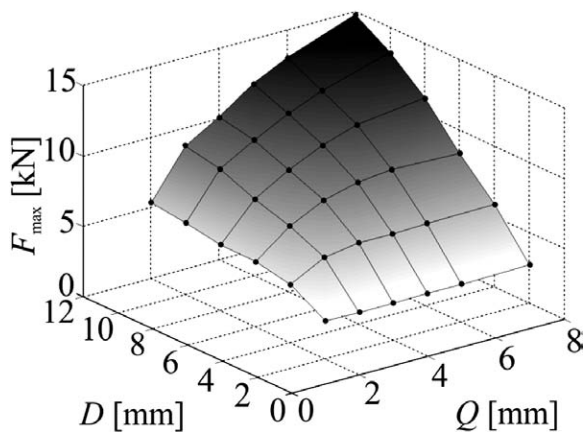


**Figure 10:** Load capacity of the pin joint for  $H = 4.6$  mm  
**Slika 10:** Nosilnost zatičnega spoja za  $H = 4,6$  mm

The influence of  $E/D$  and  $W/D$  ratios on the joint load capacity is apparent from **Figure 8**.

In these analyses, the width of the sides in the longitudinal direction  $Q_E$  and the width of the sides in the transverse direction  $Q_W$  are considered to be identical:  $Q_E = Q_W = Q$ . The range of the investigated parameters is obvious from **Figures 9, 10** and **11**. The values of the constant parameters are presented in the captions of the figures.

A gradual linearization of the dependence of the load capacity of the joint on its thickness  $H$  occurs when the width of sides  $Q$  (**Figure 9**) increases. The influence of the width of sides  $Q$  increases with the increasing pin diameter  $D$ . The influence of the width of sides  $Q$  is significant only up to the determined values of this parameter, e.g., in the case when the diameter  $D = 4$  mm, up to the value of  $Q = 3$  mm (**Figure 10**).

#### 4 CONCLUSION

The influence of geometric parameters of a pin joint on its load capacity was investigated. Experimental

dependencies of the specimen load capacity on the  $E/D$  and  $W/D$  ratios were determined.

A material model with a non-linear function with a constant asymptote was used for a description of the shear-stress behaviour. A progressive failure model was integrated in the Abaqus FEM system.

The gradual linearization of the dependence of the load capacity of the joint on its thickness  $H$  occurs when the width of sides  $Q$  increases. The influence of the width of sides  $Q$  increases with the increasing pin diameter  $D$ . The influence of the width of sides  $Q$  is significant only up to the determined values of this parameter.

In the case of the bearing-failure mechanism, the ultimate failure did not occur. Therefore, for safety reason, it is advantageous to design the pin-joint geometry so that the bearing mode occurs.

#### Acknowledgement

The work was supported by the European Regional Development Fund (ERDF), within project "NTIS – New Technologies for Information Society", European Centre of Excellence, CZ.1.05/1.1.00/02.0090 and a project of the Grant Agency of the Czech Republic, No. GAČR P101/11/0288.

#### 5 REFERENCES

- <sup>1</sup> A. Aktas, M. D. Honsu, *Composite Science and Technology*, 64 (2004), 1605–1611
- <sup>2</sup> J. Krystek, T. Kroupa, R. Kottner, Identification of mechanical properties from tensile and compression tests of unidirectional carbon composite, 48<sup>th</sup> International Scientific Conference proceedings: Experimental Stress Analysis 2010, Palacky University, 2010, 193–200
- <sup>3</sup> V. Laš, R. Zemčík, *Journal of Composite Materials*, 42 (2008) 1, 25–44
- <sup>4</sup> C. T. McCarthy, R. M. O'Higgins, R. M. Fritzzell, *Composite Structures*, 92 (2010), 173–181
- <sup>5</sup> Z. Hashin, *ASME Journal of Applied Mechanics*, 47 (1980) 2, 329–334